Validation of full-f global gyrokinetic modeling results against the FT-2 tokamak Doppler reflectometry data using synthetic diagnostics

E.Z. Gusakov[1], A.B. Altukhov[1], A.D. Gurchenko[1], S. Heuraux[2], M.A. Irzak[1], L.A. Esipov[1], T.P. Kiviniemi[3], O.L. Krutkin[1, 2], C. Lechte[4], S. Leerink[3], P. Niskala[3], G. Zadvitskiy[2]

[1]*Ioffe Institute, St Petersburg, Russia*

[2]*Institut Jean Lamour UMR 7198 CNRS, Univ. de Lorraine, BP 50840, 54011 Nancy, France*

[3] *Aalto University, Espoo, Finland*

[4] *Institute of Interfacial Process Eng. and Plasma Technology, 70569 Stuttgart, Germany*

Introduction

The anomalous energy transport remains one of the main issues in magnetic confinement fusion research. According to the present day understanding [1, 2] the anomalous transport is determined by the multi-scale drift-wave turbulence and the nonlinear interaction of its components. The gyrokinetic (GK) simulations [3, 4] provide an efficient tool for studying the nonlinear turbulent plasma dynamics and in the recent papers [5, 6] such simulations of the electron and ion distribution functions from the first principles were performed for the small research limiter tokamak FT-2. The interplay of the multi-scale turbulence components was studied and successful quantitative comparison was presented with O-mode Doppler reflectometry (DR) and enhanced microwave scattering in the upper hybrid resonance [5, 6].

Unfortunately, the interpretation of DR data is complicated due to the contribution of the poorly localized small-angle scattering, which can lead to the overestimation of the turbulence radial correlation length in the linear scattering regime [7, 8], and to its underestimation in the strongly nonlinear regime [9]. In the latter case the turbulence wavenumber spectrum measurements are questionable, and only the plasma turbulence mean velocity could be determined [10]. Moreover the 2D propagation effects additionally complicate the experimental data interpretation and its comparison with the theory predictions.

To overcome these issues, synthetic diagnostic can be used both for the interpretation of the experimental results and for the code benchmarking [11, 12]. In this paper two versions of the X-mode DR synthetic diagnostics are compared in the framework of the ELMFIRE global GK modeling of the FT-2 tokamak ohmic discharge [6]. The X-mode DR signal is computed both in the linear theory approximation using the reciprocity theorem [13] and by the full-wave code IPF-FD3D [14]. The temporal behavior of the DR signal frequency spectra and the dependence of its amplitude, frequency shift and shape on the probing antenna position are computed and compared to those measured in the experiment at the FT-2 tokamak. In the case of multi-frequency probing the radial correlation (RC) DR cross-correlation function (CCF) is also determined by both of the synthetic diagnostics and compared to that obtained in the experiment.

The experimental approach

The experiment was performed at the FT-2 tokamak (the major radius $R = 0{,}55$ m, the limiter radius $a = 0{,}079$ m) in the hydrogen ohmic discharge (with plasma current $I_p = 19$ kA, central density $n_e(0) = 4\times10^{19}$ m^{-3} and electron temperature $T_e = 470$ eV). The discharge is similar to that utilized for successful comprehensive benchmarking of the ELMFIRE GK code in [5, 6], expect for the toroidal magnetic field ($B_t(0) = 1.7$ T instead of 2.1 T). The measured electron density and temperature profiles for this discharge used in the GK modelling, as well as the ion temperature profile are shown in Fig. 1. The vertically movable (by ±2 cm) X-mode double antenna set (shown in Fig.2) installed at high magnetic field side in the vicinity of equatorial plane allowed plasma probing at variable incidence angle with frequencies in the range $f_i = (50\text{-}75)$ GHz. It was used both in DR measurements utilizing the quadrature scheme and in the RCDR technique [15], as described in [16].

In the latter case the reference channel generator was tuned to the master frequency $f_0 = 70$ GHz determining the measurement position in the vicinity of $r = 5$ cm, whereas another generator was used in the second, channel to determine the turbulence two-point CCF.

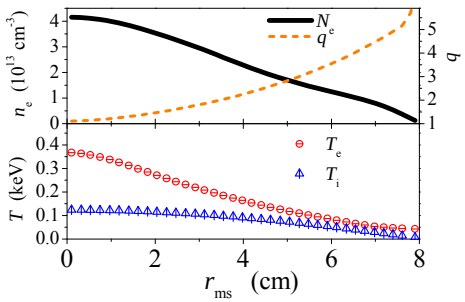

FIG.1. The discharge parameter profiles. Density – solid curve; safety factor – dashed curve. Electron temperature – circles; ion temperature – triangles.

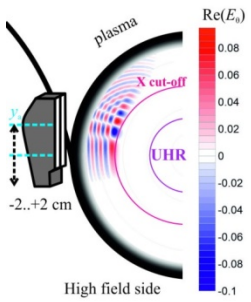

FIG.2. The DR experiment geometry and the probing wave poloidal electric field distribution computed at y_a=1.5cm.

The GK computation approach and the synthetic diagnostics

The simulations are performed with the global electrostatic particle-in-cell code ELMFIRE [3]. The simulation geometry has a circular cross-section and covers the whole radial range. The time step is set to $\delta t = 30$ ns and spatial grid to 110×8 cells in radial (r) and toroidal (φ) directions while the number of cells in poloidal (θ) direction is set to increase with r up to 950 at r=7 cm. The corresponding computational grid cell sizes at the minor radius r=5 cm are 0.07cm in radial and poloidal directions. They are sufficient for an adequate description of fluctuations contributing to the experimental DR signal, however, not for the modelling of smaller-scale turbulence, in particular, belonging to the Electron Temperature Gradient (ETG).

The "fast" synthetic X-mode DR diagnostics developed for this code [13] is based on the reciprocity theorem of electrodynamics [17] relating the high-frequency current in the plasma volume and the signal radiated by it and received by the antenna. The probing and backscattering wave propagation in the plasma not perturbed by turbulence is described in the fast synthetic diagnostic by full-wave code WaveTOP2D [18]. It should be mentioned, however, that this approach neglects the perturbations of the probing wave propagation which makes it equivalent to the linear (Born) approximation in the fluctuation amplitude. The benefit of this approach is the high speed of computations, whereas the drawback is the neglecting of the nonlinear effects.

The alternative "slow" DR synthetic diagnostic is free from this drawback. It is based on the full-wave code IPF-FD3D describing the probing and scattered wave propagation in turbulent plasma [14].

Comparison of DR frequency and turbulence poloidal wavenumber spectra

The DR spectra obtained in the experiment and provided by the synthetic diagnostics are plotted in Fig. 3 for vertical antenna shifts of different sign and value and a reasonable agreement can be seen. The meaningful difference in spectral shift is only observed at the largest antenna displacement $y_a = \pm 2.0$ cm. This difference is probably due to a contribution of experimental spectrum wings opposite to the frequency shift becoming especially heavy at high antenna displacement. This wing is opposite to the mean frequency shift of the spectrum and, presumably, is caused by small-scale drift modes, which rotate in the direction of the ion diamagnetic drift and are not

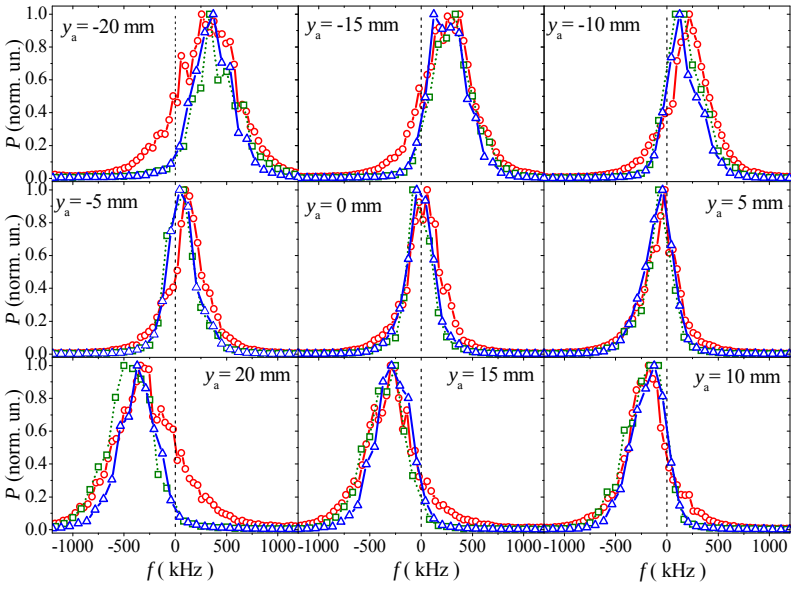

FIG.3 Comparison of DR spectra for different antenna vertical displacement. Circles –experiment; triangles – fast synthetic DR, squares – full-wave synthetic DR.

described well by the GK code.

Good agreement is confirmed by Fig. 4 and Fig. 5, where the mean frequency shift and the mean frequency width of the experimental and synthetic spectra obtained as the first and the second moment of the spectrum, respectively, are plotted as functions of the antenna vertical displacement and the turbulence poloidal wavenumber. Fig. 4 allows us to obtain estimations for the fluctuation poloidal velocity. The estimation of the mean fluctuation poloidal velocity in experiment is given by $v_\theta = \pi f_D / k_\theta \approx 2.1 \pm 0.2$ km/s, whereas the synthetic DR results in $v_\theta \approx 2.0 \pm 0.1$ km/s for the fast diagnostics and $v_\theta \approx 2.4 \pm 0.1$ km/s for the full-wave one. Fig. 5 shows the mean width of synthetic spectra to be systematically smaller than in experiment which can be attributed to the contribution of the spectral wings, which are higher in the experiment. The large backscattering spectrum width observed in Fig.5 is partly associated with strong plasma potential oscillations caused by geodesic acoustic mode (GAM) excited in the FT-2 plasma [5, 6, 19]. These oscillations could be extracted from the temporal behavior of the DR spectrum frequency shift [20].

Utilizing experimental and synthetic DR signals oscillations of the plasma poloidal velocity $v_\theta(t)$ caused by the GAM are obtained (Fig. 6). The velocity oscillation amplitudes provided by the experimental measurement, fast and full-wave synthetic diagnostics, direct GK code results are close (1.7±0.3 km/s; 1.6±0.3 km/s, 1.4±0.2 km/s and 1.3±0.5 km/s respectively). The standard deviations of the velocity fluctuations determined using DR data are also similar: the values 1.1 km/s; 0.9 km/s, 1.0 km/s and 0.8 km/s were obtained in experiment, given by the two synthetic diagnostics and directly provided by the GK code. Finally GAM frequencies provided by the experimental measurement, fast and full-wave synthetic diagnostics, direct GK code results are close too (40 kHz, 45 kHz, 36 kHz and 40 kHz respectively).

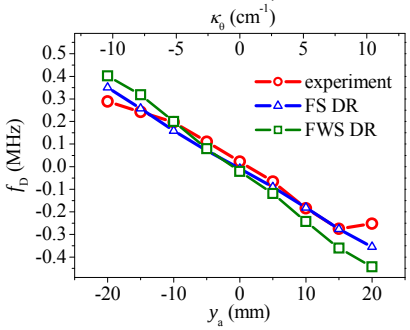

FIG. 4 Dependence of the DR signal frequency shift on the antenna vertical displacement y_a and fluctuation wavenumber. Circles – experiment; triangles – fast synthetic DR; squares full-wave synthetic DR.

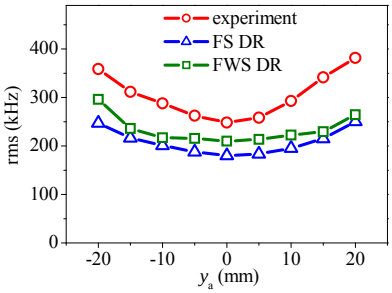

FIG. 5 Dependence of the DR signal frequency width (rms) on the antenna vertical displacement y_a. Circles –experiment; triangles – fast synthetic DR; squares full-wave synthetic DR.

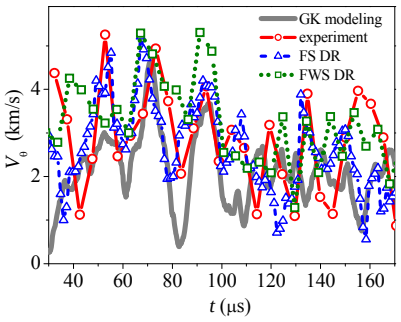

FIG. 6 Poloidal velocity temporal behavior. Thick line –computed directly by GK code, circles – measured; triangles –fast synthetic diagnostics; squares –full-wave synthetic diagnostics

Another comparison made was the DR signal power dependence on the antenna vertical displacement (Fig. 7). As it is seen in Fig.7, the decrease of the DR signal power with growing fluctuation poloidal wavenumber is substantially faster than in experiment for both synthetic diagnostics. The difference could be attributed to at least three possible reasons. The first one is related to incorrect modeling of ETG mode-scale fluctuations nonlinearly leading to an underestimation of the turbulence poloidal wavenumber spectrum in the intermediate-scale domain $\kappa_\vartheta \simeq 10 cm^{-1}$. The second reason is a possible underestimation by the GK code of the total density fluctuation level. The final reason is neglecting multiple wave reflections between the cutoff and the antenna taking place at the equatorial probing in synthetic diagnostics.

RCDR CCF comparison

Inspired by a reasonable agreement of the experimental and synthetic DR spectral data we have performed the comparison of the computed and measured RCDR CCFs for antenna displacement of +2.0 cm. The corresponding CCFs as well as density fluctuations two-point CCF for frequency f_s-f_i= *300 kHz* from GK data are plotted at Fig.8. The slow decay of the CCF

provided by fast synthetic diagnostics is most likely due to the small-angle-scattering effects [7] and neglecting strong probing wave phase modulation [9, 10, 21] coming into play with growing turbulence level. Both synthetic CCFs might also be wider due to the GK code spatial grid limitations leading to an underestimation of the turbulence radial wavenumber spectrum width, and thus – to the overestimation of the RCDR CCF width. The CCF provided by the full-wave synthetic diagnostics is much closer to the experimental one, which shows that the second reason mentioned above probably plays a minor role.

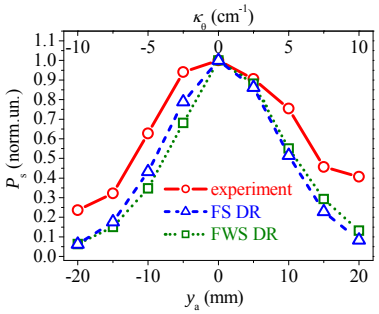

FIG. 7. Dependence of the backscattering power on the fluctuation poloidal wavenumber. Circles –experiment; triangles – fast synthetic DR; squares – full-wave synthetic DR.

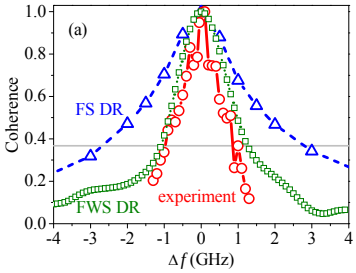

FIG. 8a The RCDR CCF against the channel frequency separation. Triangles – fast synthetic DR; squares – full-wave synthetic DR; circles – experiment.

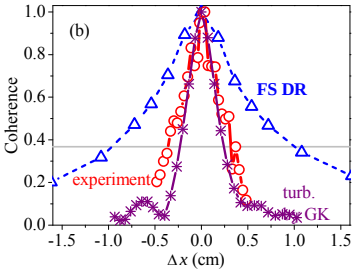

FIG. 8b The RCDR CCF against the turning point radial separation. Triangles – fast synthetic DR; circles – experiment; double crosses – turbulence CCF by GK code.

Conclusions

ELMFIRE code benchmarking against the FT-2 X-mode Doppler reflectometry experimental data utilising the fast linear and full-wave DR synthetic diagnostics has demonstrated a good agreement between the measured and computed DR frequency spectra. However, the variation of the DR signal power with growing incidence angles in experiment is slower than that predicted by both of the synthetic diagnostics. Possible explanations were suggested. The difference was also found in the decay of the DR signal CCFs with growing frequency separation. The quick decrease of the RCDR coherence observed in the experiment and full-wave synthetic diagnostic compared to the fast synthetic RCDR is attributed to nonlinear effects.

Acknowledgements

The financial support of the Russian Science Foundation grant 17-12-01110 is acknowledged. The work has been supported by the Academy of Finland grants 278487, 296853 and 318314. CSC – IT Center for Science is acknowledged for generous allocation of computational resources for this work. The FT-2 tokamak maintenance was supported by Ioffe Institute whereas M.A. Irzak acknowledges the support of Russian Academy of Science Presidium program.

References

1. P.H. DIAMOND et al., Plasma Phys. Control. Fusion **47**, R35 (2005).
2. P.W. TERRY, Reviews of Modern Physics **72**, 109 (2000).
3. J.A. HEIKKINEN et al., J. Comp. Phys. **227**, 5582 (2008).
4. Y. SARAZIN et al., Nucl. Fusion 51, 103023 (2011).
5. S LEERINK et al., Phys. Rev. Lett., **109** 165001, (2012).
6. E.Z. GUSAKOV, A.B. ALTUKHOV, V.V. BULANIN et al. *Plasma Phys. Control. Fusion*, **55,** 124034 (2013).
7. E GUSAKOV, M IRZAK AND A POPOV Plasma Phys. Control. Fusion **56,** 025009 (2014).
8. E GUSAKOV, M IRZAK, A POPOV et al. Physics of Plasmas **24**, 022119 (2017).
9. E.Z. GUSAKOV, A.YU. POPOV, Plasma Phys. Control. Fusion **46,** 1393 (2004).
10. E.Z. GUSAKOV,A.V. SURKOV, A.YU. POPOV, Plasma Phys. Control. Fusion **47,** 959 (2005).
11. S. Hacquin et al., Phys. Plasmas 23 (2016) 092303
12. J. Citrin et al., Phys. Plasmas Control. Fusion 59 (2017) 064010
13. A. B. ALTUKHOV, A. D. GURCHENKO, E. Z. GUSAKOV et.al. Phys. Plasmas **25**, 082305 (2018).
14. LECHTE C et al. Plasma Phys Control. Fusion **59,** 07500 (2017).
15. SCHIRMER J et al. Plasma Phys. Control. Fusion **49** 1019 (2007).
16. ALTUKHOV A.B., GURCHENKO A.D. et al. Plasma Phys. and Controlled Fusion **58,** 105004 (2016).
17. A. D. PILIYA, A. YU. POPOV, Plasma Phys. Control. Fusion **44**, 467 (2002).
18. E.Z. GUSAKOV, V.V. DYACHENKO, M.A. IRZAK et al. Plasma Phys. Control. Fusion 52, 075018 (2010).
19. A D GURCHENKO, E Z GUSAKOV, A B ALTUKHOV et al. PPCF **55,** 085017 (2013).
20. CONWAY A.D., SCOTT B., SCHIRMER J. et al. Plasma Phys. Control. Fusion **47,** 1165 (2005).
21. E.Z. GUSAKOV, A.YU. POPOV, Plasma Phys. and Control. Fusion, v.**44**, No 11, p.2327 (2002)